Convergent Zone-Refinement Method for Risk Assessment of Gas Turbine Disks Subject to Low-Frequency Metallurgical Defects

Harry R. Millwater
Department of Mechanical Engineering,
The University of Texas at San Antonio,
One UTSA Circle,
San Antonio, TX, 78249
e-mail: harry.millwater@utsa.edu

Michael P. Enright
Reliability and Material Integrity,
Southwest Research Institute,
6220 Culebra Rd.,
San Antonio, TX, 78228
e-mail: menright@swri.org

Simeon H. K. Fitch
Mustard Seed Software,
1634 Brandywine Drive,
Charlottesville, VA, 22901
e-mail: simeon.fitch@mseedsoft.com

Titanium gas turbine disks are subject to a rare but not insignificant probability of fracture due to metallurgical defects, particularly hard α. A probabilistic methodology has been developed and implemented in concordance with the Federal Aviation Administration (FAA) Advisory Circular 33.14-1 to compute the probability of fracture of gas turbine titanium disks subject to low-frequency metallurgical (hard α) defects. This methodology is further developed here to ensure that a robust, converged, accurate calculation of the probability is computed that is independent of discretization issues. A zone-based material discretization methodology is implemented, then refined locally through further discretization using risk contribution factors as a metric. The technical approach is akin to "h" refinement in finite element analysis; that is, a local metric is used to indicate regions requiring further refinement, and subsequent refinement yields a more accurate solution. Supporting technology improvements are also discussed, including localized finite element refinement and onion skinning for zone subdivision resolution, and a restart database and parallel processing for computational efficiency. A numerical example is presented for demonstration. [DOI: 10.1115/1.2431393]

Introduction

As a result of the airliner accident at Sioux City, Iowa, in 1989 [1], where a disk rupture in the tail engine caused the loss of hydraulics and subsequent crash of the plane, the FAA requested in 1991 that industry, through the Aerospace Industries Association, review available techniques to determine whether a probabilistic damage tolerance approach could be introduced to reduce the rate of uncontained rotor events. In this case, the titanium fan disk fractured due to a crack that initiated from a hard α defect formed during the titanium melt and not detected during in-service inspections. The industry working group concluded that additional enhancements to the conventional rotor life management methodology could be established which explicitly address anomalous conditions.

The Federal Aviation Adminstration (FAA), with industry input, has developed an advisory circular (AC 33.14-1) [2] that, among other things, outlines a probabilistic damage tolerance analysis methodology for assessing the risk of fracture of titanium rotors on gas turbine engines. The probabilistic methodology complements and does not replace preexisting approaches.

The advisory circular (AC) advises that all new titanium rotors be designed such that the probability of fracture (POF) per flight is less than the design target risk (DTR). The DTR is the standard against which probabilistic risk assessment results (stated in terms of component event rates and engine level event rates) are compared. The DTR is currently set at 10^{-9} for the component event rate and 5×10^{-9} for the engine event rate, i.e., the average probability of fracture per flight over the life of the titanium component should be $<10^{-9}$ and the cumulative average probability of fracture per flight over the life of all engine titanium components should be less than 5×10^{-9}. A new engine design is expected to meet the DTR before the engine is certified.

The probabilistic damage tolerance requirement for hard α defects is a recent development and, as such, methodologies to quantify the POF are also fairly recent. A methodology for high-frequency anomalies in nickel-based powder metal components has been developed and validated by comparison to seeded fracture specimens [3]. Although developed for powder nickel, the probabilistic equations will reduce to the simpler form described in the AC and implemented here; however, the computational strategy for solving the equations is different.

The advisory circular specifies one approach to quantifying the POF. This methodology is based on discretizing the disk structure into a number of zones. A zone is a grouping of material such that all locations in the zone have a generally uniform stress state, and the same fatigue crack growth properties, inspection schedules, probability of detection curves, and anomaly distribution. In other words, the risk computed for any subregion of material of the zone will be the same or nearly so, and therefore, the risk is assumed constant for a defect located anywhere in that zone. Since there will be some variation in calculated POF, depending on the location of the defect within a zone, a conservative approach is specified whereby the defect is placed in the life-limiting location, i.e., the location within the zone that will yield the highest POF. The finite element mesh and stress results are used as the framework to select zone boundaries and, hence, the zone discretization.

The FAA has funded a research program in consort with several commercial engine original equipment manufacturers and research organizations to develop computational techniques and software to quantify the POF due to hard α defects in titanium based on the methodology outlined in the AC. The probabilistic methodology from this research program is outlined below and discussed in detail in [4,5]. Subsequent work is ongoing to extend

Submitted to ASME for publication in the JOURNAL OF ENGINEERING FOR GAS TURBINES AND POWER. Manuscript received March 8, 2005; final manuscript received September 15, 2006. Review conducted by Marc P. Mignolet.

the technology and apply the methodology to materials with more frequent defects such as powder nickel and materials with surface defects [6].

The zone-based methodology is clearly dependent on the discretization of the material into zones. The purpose of this research is to provide an extension to the probabilistic algorithm outlined in the AC to ensure that a converged risk solution is obtained regardless of the initial zone discretization. This is accomplished through the application of an iterative discretization refinement methodology akin to the "h" refinement method in finite element analysis, with critical components being: the criteria for determining regions of discretization, efficiently developing a refined model, and efficiently calculating an updated solution. The methodology is demonstrated through the analysis of an impeller disk.

Methodology Overview: A Zone-Based Approach

Probabilistic Methodology. Oftentimes, the critical locations of a structure are known a priori; typically, these locations are the highly stressed areas. However, since metallurgical defects are induced during the material melting process, defects may be randomly distributed within a disk. Thus, the location of a defect is a random variable. This fact considerably complicates a probabilistic analysis of a titanium structural component.

The random location of a defect in the cross section could be simulated using Monte Carlo sampling, that is, by randomly distributing the defect locations; however, an acceptance-rejection method would most likely be required since a disk cross section is irregular. One difficulty with this approach is that a large number of samples, e.g., several to many millions, would be required to ensure that all significant regions of the disk are sampled. For example, a highly stressed region near a notch would have a significant risk contribution but only a small volume and, therefore, may not be sampled sufficiently since the probability of locating samples within that region would be small. A second difficulty is that for each location the stress history must be obtained, typically from a finite element (FE) model, and processed to obtain the damaging fatigue cycles, i.e., rainflow cycle counting [7]. This operation would be very computationally demanding if carried out at every sample location.

An alternate approach is to adopt a "stratified sampling-like" method whereby the user divides the domain into regions (hereafter called "zones"), and sampling is performed in each region. This insures that every region defined by the user will be sampled. Thus, the user can tailor the sampling based on a priori knowledge about the likely high-risk regions of the disk. This leads to an efficient probabilistic approach; however, this leaves the accuracy of the result dependent on the user's definition of zones.

The second component of the alternate approach is to locate all defects placed within a zone at a single location in the zone and the cycles-to-failure and risk results for that location are assumed representative of a defect located anywhere in the zone. Thus, the stress information is retrieved and processed only once for all samples within a zone, resulting in a considerable savings in computer time. The location recommended in the AC is the life-limiting location of the zone, i.e., the location in the zone from which the cycles to failure will be the lowest. If the defect is located in the life-limiting location, the risk computed will be a conservative estimate of the risk for the zone.

The selection of the life-limiting location in a zone is not known a priori but can be determined by performing deterministic fatigue calculations for several candidate locations. In general, the stress and the proximity to a structural boundary are the two dominant considerations.

The methodology assumes a low frequency of anomalies; at most, only one significant anomaly exists in the disk; hence, the probability of two or more anomalies in a disk is negligible. This is consistent with the frequency of hard α defects in rotor-grade titanium [4,8]. For materials with more frequent anomalies (e.g., powder nickel), a Poisson distribution can be used to model the probability of occurrence with subsequent modifications in the probability equations [3,6,9].

The zone-based methodology accounts for:

- the probability of having an anomaly in the disk
- the probability that a hard α anomaly developed during the titanium melt process could be in any location of the disk
- the initial size distribution of the anomaly
- randomness in the time of inspection time, probability of detection, finite element stresses and fracture mechanics analysis
- the probability of fracture if an anomaly exists
- the probability of detecting an anomaly before the disk has fractured

The probability of fracture of the zones are modeled as independent events. The probability of fracture of the disk can be obtained from the system reliability equation

$$P[\text{disk}] = P[\text{fracture in any zone}] = P[F_1 \cup F_2 \cup \cdots \cup F_N] = 1 - \prod_{i=1}^{n} (1 - P[F_i]) \approx \sum_{i=1}^{n} P[F_i] \quad (1)$$

where F_i indicates fracture of a defect originating in zone i, $P[F_i]$ indicates the probability of fracture of an initial defect located in zone i, N is the total number of zones, $\cup$ is the union logical operator, and the approximate equality occurs because $P[F_i]$ is small.

The probability of fracture of a zone, i.e., $P[F_i]$ requires an anomaly be present and grow to failure. This can be represented as

$$P[F_i] = P[A_i]P[B_i|A_i] \quad (2)$$

where $P[A_i]$ is the probability of having an anomaly in zone i and $P[B_i|A_i]$ is the conditional probability of fracture given an anomaly in zone i.

The probability of a hard α defect being present per volume of material is dependent on the procedure used during the melting of the titanium and the inspection procedures used on the billet. Industry-developed exceedance curves define the frequency of occurrence and size of hard α defects [8]. The probability of having a defect in a zone, i.e., $P[A_i]$, is a function of the ratio of the zone volume to the volume of material used as a reference in developing the exceedance curve.

The conditional probability $P[B_i|A_i]$ is computed using probabilistic fracture-mechanics-based life assessment for low-cycle fatigue. The hard α phase anomalies found in titanium materials are typically brittle [4,8], and may form into growing cracks as early as the first cycle of applied load. For conservative fracture mechanics predictions, it is assumed that a crack forms at cycle zero, i.e., the crack initiation time is zero. Therefore, the cycles to failure is estimated exclusively using a crack propagation algorithm. The effects of inspections on the conditional POF can be determined by altering the conditional probability through the simulation of in-service inspections using anomaly detection and removal calculations based on crack size distributions and probability-of-detection curves [10]. The conditional probability calculations are computed using Monte Carlo sampling or importance sampling [11].

Fracture Mechanics Model. Evaluation of fatigue life requires calculation of stress intensity factors (SIFs) as a function of crack size. Calculation of SIFs for an arbitrary crack and structural geometry and stresses using finite or boundary element formulations are possible but not practical for probabilistic fatigue calculations. A practical yet reasonably accurate approach is to use weight functions [12,13]. Weight function methods for SIF determination require as input, the stress normal to the crack plane and the

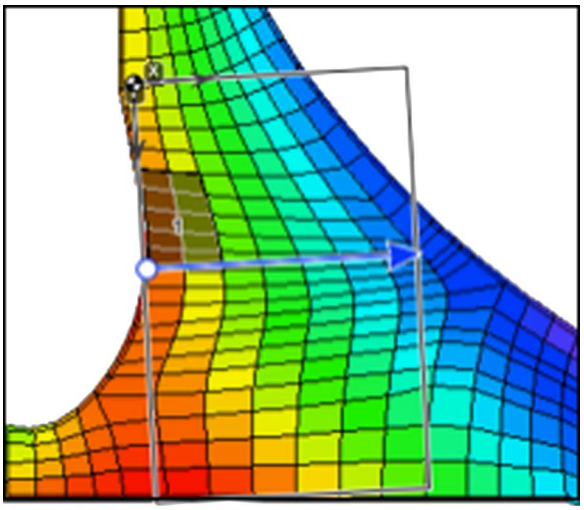

Fig. 1 Fracture mechanics model using a rectangular plate overlaid on an axisymmetric finite element model

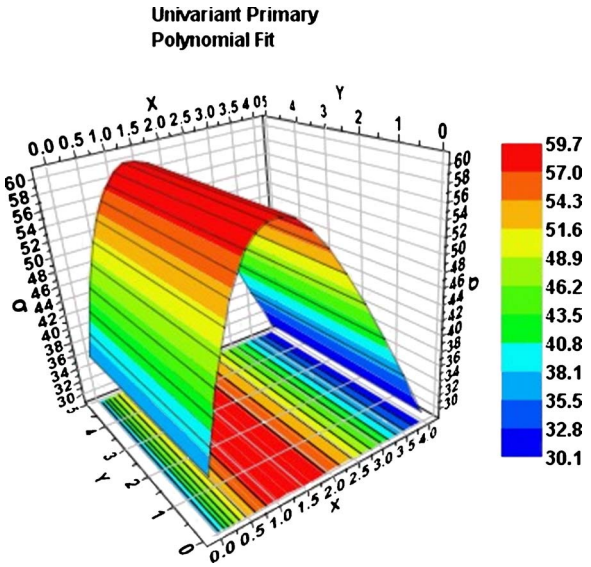

Fig. 2 Univariant stress gradient

geometric boundaries of the *uncracked* body. This allows one finite element solution to be used for all crack sizes. Univariant gradients and sometimes bivariant gradients in the stress field can be accommodated.

Weight functions have been developed for rectangular plate geometries and used as a surrogate for the more complex actual geometry [14]. This approximation is often sufficient because the SIF is only weakly affected by the boundary until the boundary is very close. During modeling, for each zone, the user defines a rectangular plate relative to the crack location and the boundaries of the actual part. Figure 1 shows the crack (white circle), the zone material (highlighted elements), the rectangular plate model (boundaries marked by black line), and the stress gradient direction (blue arrow), overlaid on a finite element model that is color coded based on the value of tangential stress. The crack is placed in the highest stressed location of the zone material, which is estimated to be the life-limiting location.

Selection of a rectangular plate that can adequately approximate the disk boundaries is subjective. A conservative approach can be chosen by making the plate boundaries smaller than the actual boundary and thus calculating a larger SIF and, hence, lower life estimate. Since the SIF is only weakly affected by the boundary proximity, approximating the boundary near the crack is most important.

The "gradient" vector shown in Fig. 1 indicates the direction along which the stress normal to the fracture plane is extracted from the FE results and used to construct a univariant gradient stress field normal to the fracture plane, as shown in Fig. 2. The vector does not restrict crack growth in any direction but only defines the direction in which a stress gradient will be considered when determining the stress intensity factor.

The gradient vector must not extend beyond the edges of the FE model in order to extract stresses along the vector. As such, a "clipping" algorithm is implemented within the graphical user interface to ensure this condition is satisfied; that is, the intersections of the vector and the disk boundaries are computed and, if necessary, the ends of the plate are automatically adjusted to ensure the vector lies within the disk geometry. The user has freedom to define the plate orientation and dimensions with the one restriction that the entire gradient vector must lie entirely within the FE model.

Random Variables. The random variables considered in the analysis are shown in Table 1. The anomaly location is addressed by the zone methodology discussed previously. The anomaly distribution defines the probability of having an anomaly and the size distribution of the anomalies. The FAA advisory circular provides industry-developed anomaly distributions based on melting practice and forging inspection processes [8]. The Aerospace Industries Association, Rotor Integrity Subcommittee, periodically updates the anomaly distributions. Variations in time of inspection are used to model real-world uncertainties in the inspection of a fleet of engines. The probability of detection defines the expected probability of detecting an anomaly as a function of anomaly size and inspection method.

Variations in finite element stress results are simulated using a multiplier that can be considered random, i.e.,

$$\sigma = \sigma(\mathrm{FE})S \tag{3}$$

where $\sigma(\mathrm{FE})$ are the stresses obtained from the finite element analysis and S is a random variable modeled with a lognormal distribution.

A life scatter factor is implemented to consider variations in predicted cycles to failure, i.e.,

$$N = N(FM)B \tag{4}$$

where $N(FM)$ is the predicted cycles to failure from fracture mechanics analysis and B is a random variable modeled with a lognormal distribution. The life-scatter random variable encompasses all forms of variation in the computed cycles to failure with respect to the actual cycles to failure, such as material crack growth rate variation, stress intensity factor idealizations, etc.

Recent work has expanded the random variables that can be considered through application of a generalized conditional expectation method [15,16]. Thus, the zone-based methodology can be utilized with additional random variables such as geometric, loading, and material properties.

Convergent Zone Refinement Methodology

The risk solution obtained from the zone-based methodology is dependent on the discretization of the risk zones, i.e., the size and

Table 1 Random variables considered

Anomaly location
Anomaly distribution (size and frequency)
Time of inspection
Probability of detection
Finite element stress scatter
Life scatter (fracture mechanics multiplier)

Table 2 Zone refinement methodology

No.	Step details	Operator[a]
1	User defines initial zones and sets parameters—convergence criteria, maximum limits	U
2	Risk assessment evaluated	C
3	Examine stop criteria a. Risk $\leq$ risk limit, stop analysis b. Relative change in disk risk $<$ change limit, stop analysis c. All risk contribution factor (RCF) values $<$ RCF limit d. Maximum cpu time reached	U
4	Select zones to be refined based upon the zone risk contribution factor—with or without inspection a. Zone RCF $<$ RCF factor limit, no refinement b. Zone RCF $\geq$ RCF limit, refine into subzones	U
5	Generate potential subzones a. Determine material in each subzone i. Use stress centroid equation ii. Embedded—create four or three subzones iii. Surface—create two subzones b. Place flaw in each subzone geometrically closest to flaw in parent zone c. Define plate for each subzone Parent plate orientation, size and location used as default d. Inherit properties from parent Gradient direction, volume multiplier, inspection schedules, material no., crack type, crack plane, anomaly distribution, # samples	C
6	Read risk results from unchanged zones from database	C
7	Compute risk for new zones, combine with unaltered zones, that is, return to step 2	C

[a]U and C denote User and Computer, respectively.

number of zones. The methodology does, however, require that the flaw be placed in the life-limiting location of the zone; the calculated risk is, therefore, greater for coarse discretizations compared to fine zone discretizations. In other words, the risk should be reduced as the number of zones is increased.

A methodology is presented that provides a converged risk solution independent of the initial discretization of zones. The features of the algorithm are

- Robust—will work for any well-posed problem
- Convergent—will converge to correct solution
- Simple—easy to understand, not hidden nor confusing
- Stable—risk solution is not dependent on the initial zone breakup

The detailed zone refinement methodology is shown in Table 2. Steps 3–7 are iterated as necessary.

The iterative algorithm is implemented through a combination of user actions and computational algorithms as denoted in column 3 of Table 2 where "U" denotes a user action and "C" denotes a computational algorithm.

Selecting Zones to Refine. Identification of the zones requiring refinement (Step 4 in Table 2) is a key ingredient to the zone refinement algorithm. The computational time associated with prediction of disk risk is directly proportional to the number of zones. For optimum computational efficiency, zone refinement should be applied only to the zones that significantly influence the overall disk risk.

The risk contribution factor (RCF) for a zone indicates the risk contribution of the zone relative to the risk of the disk, given mathematically as

$$\mathrm{RCF}_i = \frac{P[F_i]}{\sum_{j=1}^{n} P[F_j]} = \frac{P[A_i]^* P[B_i|A_i]}{\sum_{j=1}^{n} P[A_j]^* P[B_j|A_j]} \tag{5}$$

where N is the total number of zones.

The risk contribution factors are defined such that

$$\sum_{i=1}^{n} \mathrm{RCF}_i = 1 \tag{6}$$

Therefore, a percent limit, (RCF limit, Table 2, Step 4), can be used to determine if a zone is significant and should be refined. Through this approach, critical zones are refined until all zones have an RCF less than an RCF limit or some other exit criterion is reached (see Step 3 in Table 2). Note, each zone has a separate RCF for analyses with or without inspections and these RCF values may not be the same. As a result, the largest RCF value from the with and without inspections results is typically used.

In Fig. 3, zones with an RCF $>5\%$ are highlighted in red (gray). These zones are candidates for zone refinement as described in Steps 4 and 5 of Table 2 and discussed below. The user can change the RCF threshold value as desired.

Zone Refinement

Partitioning Parent Zone into Subzones. The procedure to refine a zone is to first subdivide the zone area into subzones. This is shown schematically in Fig. 4. The parent zone, highlighted material on the left, is subdivided into fourths (sometimes thirds depending on the geometry) about the stress centroid of the zone

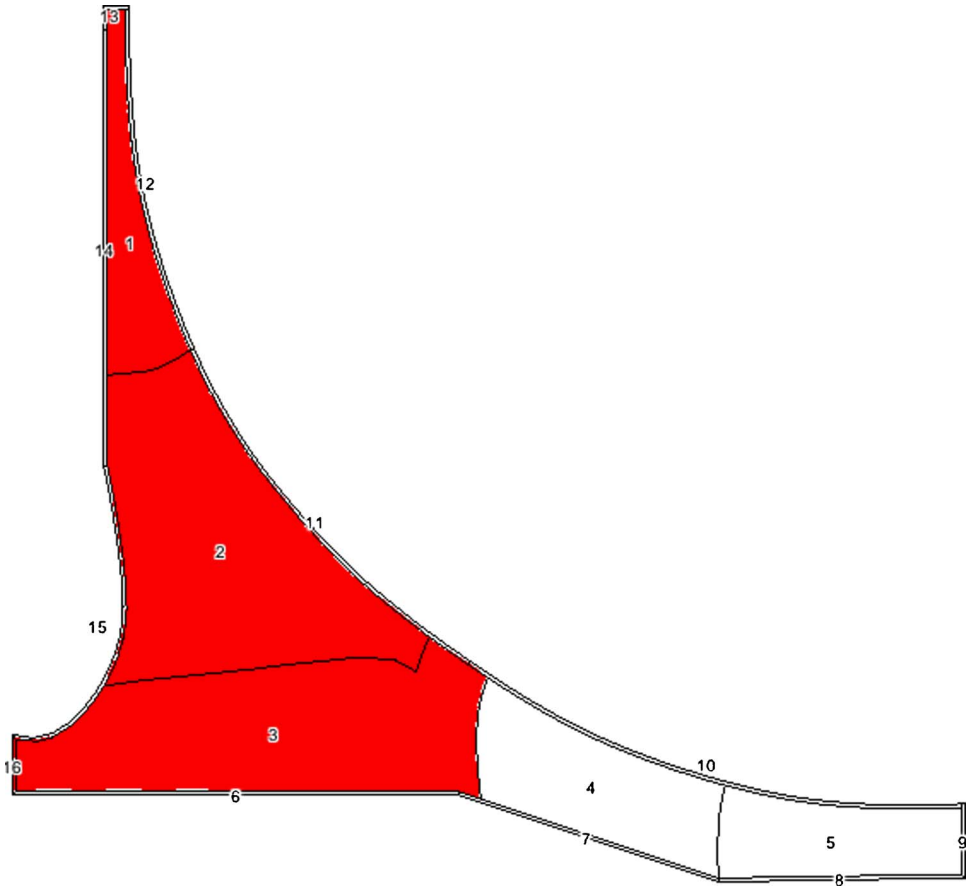

Fig. 3 Selection of zones for refinement using risk contribution factors; red (gray) zones indicate RCF greater than 5%

using the local coordinates of the plate. The stress centroid is defined by coordinates R_{cg} (radial), Z_{cg} (axial) as

$$R_{cg} = \frac{\sum_{k=1}^{K}\sum_{l=1}^{L} R_{lk}\sigma_{lk}}{\sum_{k=1}^{K}\sum_{l=1}^{L} \sigma_{lk}} \quad Z_{cg} = \frac{\sum_{k=1}^{K}\sum_{l=1}^{L} Z_{lk}\sigma_{lk}}{\sum_{k=1}^{K}\sum_{l=1}^{L} \sigma_{lk}} \tag{7}$$

where K denotes the number of finite elements in the zone to be divided, L denotes the number of nodes within element k, R_{lk} and Z_{lk} are the radial and axial locations of node l within element k, and σ_{lk} is the stress at node l within element k. Typically, the user selects the most damaging stress component and load case on which to base refinement. The advantage of using the stress centroid equation instead of the geometric equation is that the centroid will be placed closer to the highly stressed region, ensuring smaller subsequent zones within that region.

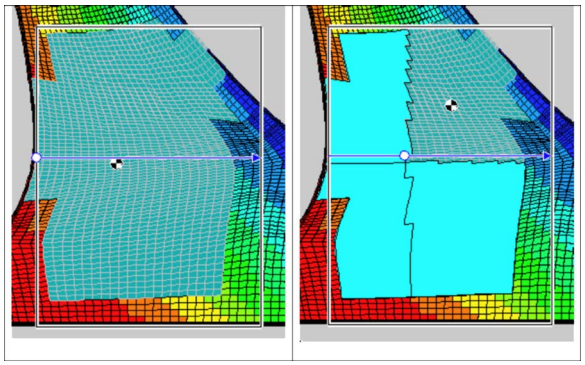

Fig. 4 Schematic of zone subdivision: parent zone (left) divided into four subzones (right) about stress centroid of parent

Once the centroid is located, the zone is bisected into two, three, or four subzones. For defects initiating in the interior of the part, i.e., embedded cracks, lines emanating from the zone's stress centroid parallel to the sides of the plate are used to determine the subzone location of each finite element based on the element's geometric centroid location relative to the lines. Generally four subzones are created, see Fig. 4; however, an oddly shaped parent zone, e.g., "L" shaped, may result in only three subzones. There is no restriction on the shape of the zones.

For defects initiating on the surface of the part, i.e., surface cracks, only a single row of elements along the surface comprises the zone. A line parallel to the side of the plate (usually normal to the surface) passing through the stress centroid is used to partition the parent zone into two subzones.

Defining Crack Location and Plate Geometry. Next, the flaw location must be specified for each subzone. For the parent zone, the flaw is by definition located in the life-limiting location. For the new subzone, it is theoretically possible to compute the life at multiple locations, say each node point within the zone, and then select the location with the lowest life. However, this solution is not executed by default due to excessive computation time. Another option is to locate the flaw at the highest stress in the zone based on the stress state from the most damaging load case. However, this option ignores the amplification effect near surfaces have on the stress intensity factor and, therefore, may not be conservative. The approach implemented is to locate the subzone flaw

within the subzone material at the geometrically closest point to the flaw location in the parent zone. This approach is predicated on the premise that the parent flaw is in the life-limiting location, which by definition, considers all factors affecting life, primarily stress level and location. The location of the flaw for the new zone is shown in the right image in Fig. 4 for the upper rightmost zone.

It is possible that the flaw location in the subzone is not the life-limiting location, particularly if a large zone is subdivided and other boundaries become important for the subzone or significant stress gradients occur within a parent zone. However, the zone-refinement scheme reduces the probability of not locating a defect in the life-limiting location because subdividing the zone reduces, typically, by a factor of four, the cross-sectional area associated with that zone, and the cycles-to-failure of a defect located anywhere in the zone becomes more homogeneous. Second, the zone-refinement scheme reduces the importance of determining the life-limiting location for any particular zone because any zone of significance is, by definition, subdivided until the RCF is below a limiting value. As such, any individual zone cannot have a dominant effect on the overall disk risk, and thus, not placing the defect in the life-limiting location in any particular zone will not grossly affect the overall disk risk calculation.

Next, a rectangular plate must be defined for the subzone for the fracture mechanics solutions. The procedure is to:

1. Use the same plate as the parent zone (assuming the new crack is inside the existing plate), and keep the same gradient direction.
2. Clip front and back along gradient line if necessary.
3. If the new flaw location is outside parent plate, then move the plate if possible. If not possible, then warn the user so that the late may be repositioning manually.

Other properties necessary for the risk analysis are inherited from the parent zone, such as material properties, inspection schedules, and anomaly distribution.

Efficient Reanalysis—Computational Issues. After subdivision of selected zones, the model is reanalyzed to determine the updated risk and RCFs. Several, if not many, of the zones will not have been altered and, therefore, have the same risk value as before. In support of reanalysis, an XML results database is used to store results by zone from a previous analysis [17]. During re-analysis, for each zone, the database is scanned in search of a matching zone. If a match is found, then the results are retrieved and analysis proceeds to the next zone. If a match is not found, then the POF for the zone is computed and the results are stored in a new database. This capability provides a large reduction in computer time versus rerunning all zones.

The zone-based methodology is defined such that the determination of the probability of fracture for the zones can be computed independently. A parallel processing spatial decomposition methodology using a network of workstations and personal computers is implemented whereby each computer analyzes a region of the disk, i.e., a single zone or a collection of zones [18]. Each analysis creates an XML database. The individual analyses are then combined by searching across all databases to obtain the probability of fracture of the disk. This methodology produces an order of magnitude or more improvement in computation time.

Supporting Technology: Element Refinement and Onion Skinning. The finite element mesh is used as a framework for determining zone boundaries. However, although atypical, situations may arise where the FE mesh is too coarse for the risk assessment. This may occur, for example, near surfaces where there is little or no stress gradient but a significant risk gradient due to the amplification effect of the near surface on the SIF. For these situations, an "element refinement" option can be used to repeatedly subdivide the FE mesh. Any nodes created are interior to existing elements; therefore, stress components for any new nodes are obtained by interpolating the stress components from the original mesh using the element shape functions.

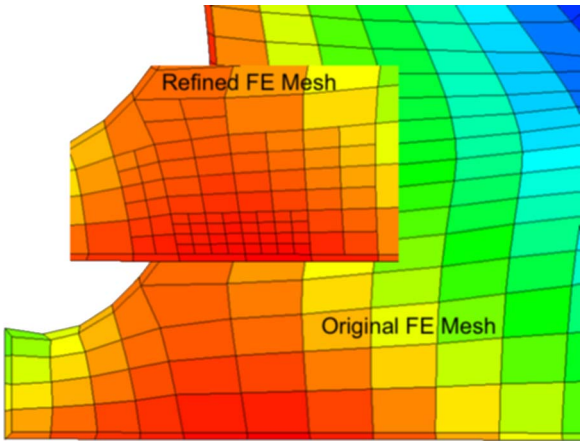

Fig. 5 Example of finite element subdivision in support of zone refinement

Figure 5 shows an example of element subdivision of a region near a surface. The FE mesh is only used to define zone boundaries; it is not used for FE analysis. Thus, there are no continuity requirements along element edges and any localized subdivision is allowed. It is assumed that the finite element model is sufficiently refined with respect to stress gradients; therefore, subdividing the elements and interpolating the stress results using element shape functions does not introduce error.

The advisory circular states that a 20 mil (0.020 in.) layer, e.g., onion skin, of material be associated with surface flaws. However, the FE mesh was most likely developed without this requirement in mind. Therefore, an algorithm has been developed and implemented to automatically create a layer of elements of the specified thickness.

The onion skinning algorithm computes a vector of the required length, e.g., δ, normal to the element edge. If the projected distance to the normal of the nearest node to the element edge is $<\delta$, no subdivision is required. If the projected distance is $>\delta$, additional nodes are located along the current element edge such that the perpendicular distance to the surface is δ. The original element is then split into two elements. Figure 6 shows an example of onion skinning. The "red" (dark gray) nodes indicate the nodes of the original element. The "green" (gray) nodes and green (gray) element side denote components generated by the onion-skinning algorithm. Elements "a" and "b" are created and the original element is deleted. Stress components and temperatures are interpolated for the new nodal points. The onion-skinning algorithm is summarized in Table 3.

Exit Criteria. The exit criteria used to terminate the iterative algorithm vary. The first criterion to examine is whether the risk

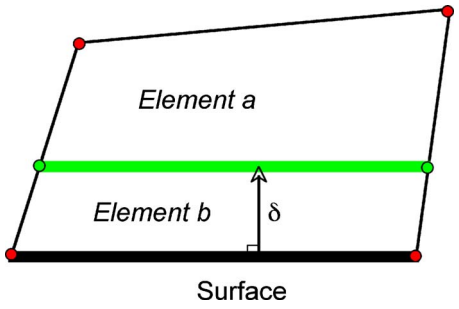

Fig. 6 Example of onion-skinning algorithm applied to a single finite element

Table 3 Onion skinning algorithm

1	User graphically selects set of elements to consider for onion skinning
2	Filter out nonsurface elements: a. Compute geometry border as set of edges b. Iterate through elements checking for an element edge in border set
3	For each selected border element: a. Create a vector normal to the surface edge with length equal to the onion skin distance δ b. Using the dot product, determine the distance along element edge that gives a normal distance to the surface equal to δ
4	Using linear interpolation between adjacent edge endpoints and the normal distance δ, compute location, temperature and stress components for new nodes
5	Delete old element and replace with two new elements using new nodes

limit, i.e., the DTR, has been satisfied. If the life-limiting location has been chosen for each zone, then the POF estimate is conservative and further zone discretization will reduce the POF. Therefore, if the POF is below the risk limit, then the design is sufficient and the algorithm can be terminated.

A second exit criterion is to examine the RCF values for all zones. If the RCF values are all below a reasonable RCF threshold, then further zone discretizations will not likely produce a significant change in the risk. An RCF threshold of 1-5% is typical. For example, if the RCF for a zone is 2%, then subdividing that zone will at most affect only 2% of the total disk risk. Summation of the risk in all zones above the RCF limit gives an indication of the total amount of disk risk that might be affected by zone refinement.

A related criterion is to examine the relative change in the risk between iterations. If the change in risk is small, then further zone discretizations will not likely produce a significant change in the risk.

A final criterion is to examine the maximum limits for the analysis, e.g., maximum number of iterations or the maximum cpu time is reached. These are practical criteria based mainly on experience.

If the risk is greater than the DTR, further refinement can be attempted to meet the target. If the target cannot be obtained, then disk redesign is required.

Numerical Example

An impeller model is used to demonstrate the algorithm. The three-dimensional model is shown in Fig. 7. Because of axisymmetry, only the cross-sectional area is discretized for finite element and risk analysis, as shown subsequently. The procedure outlined in Table 2 is performed using an RCF threshold of 5%. Any zone with an RCF of $\geq$5% for either with or without inspection is subdivided. The iterative procedure is carried out until the RCF values for all zones are $<$5%.

A refinement sequence is shown in Figs. 8(*a*)–8(*f*), starting from a very coarse 16 zone model (iteration 0) and concluding, after iteration 6, with a refined 75 zone model. (Note, there are several very thin surface zones around the boundary of the model that cannot be seen at this scale.) The zones with an RCF greater or equal to 5% are colored red (gray) and others white. The red (gray) zones are refined in the succeeding iteration.

In each iteration, the current number of total zones in the model is indicated along with the number of zones that are unchanged and, hence, retrieved from the results database. The percent time for solving that particular model relative to the total computational time for all iterations is given. Also given is the cumulative percentage of time from iteration zero. For example, the results after iteration 1 show a total of 25 zones with 13 unchanged from

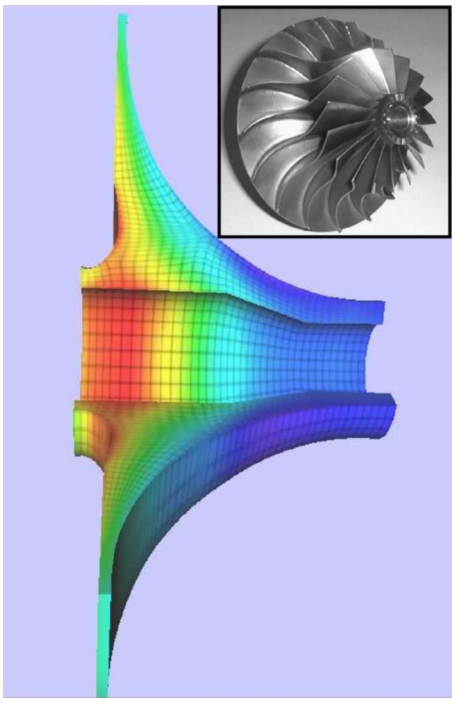

Fig. 7 Three-dimensional idealized impeller finite element model

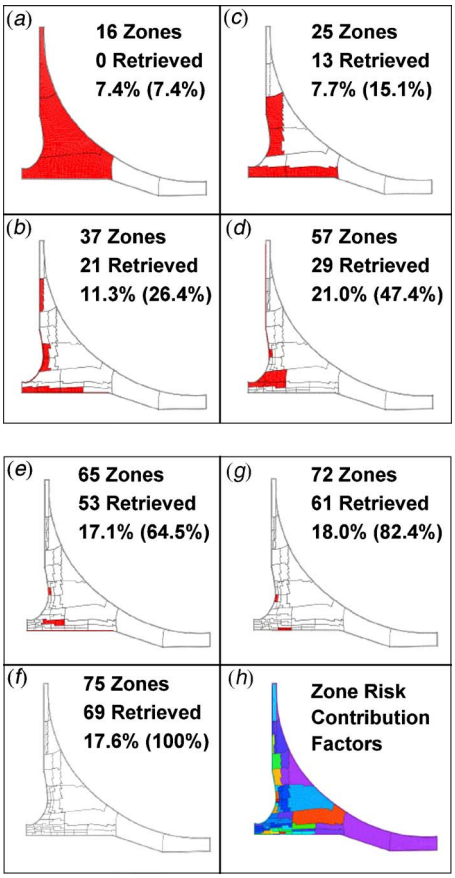

Fig. 8 (a)–(d) Sequence of zone refinement iterations for impeller rotor disk model and (e)–(h) sequence of zone refinement iterations for impeller rotor disk model

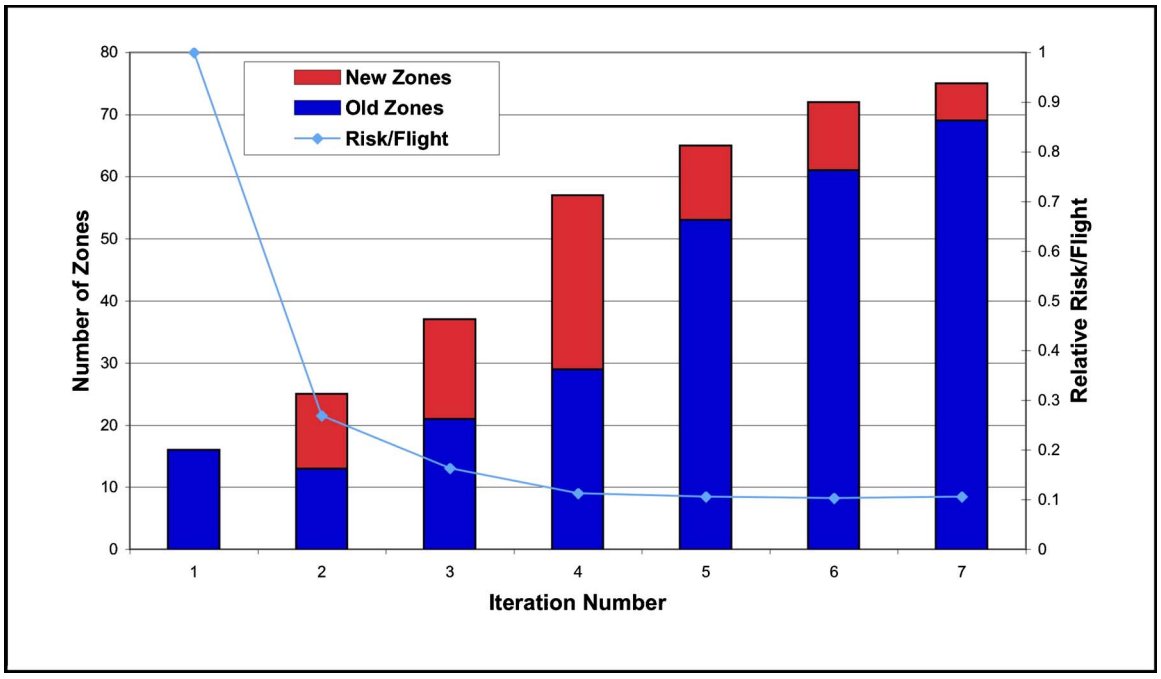

Fig. 9 Iteration results showing the convergence in risk versus the number of zones (old and new)

iteration 0. The solution time for iteration 1 is 7.7% of the total computational time. The cumulative solution time for iterations 0 and 1 is 15.1% of the total computational time.

Figure 8(*g*) shows the converged solution with the zones colored using a color map from high RCF (red) to low RCF (purple); however, all zones have an RCF of $<5\%$.

Figure 9 shows a chart of the normalized POF (normalized to the initial computed risk) versus the iteration number. Since the life-limiting location is chosen for the defect in each zone, the calculated POF is conservative and subsequent refinement reduces the POF. The results are typical; a large reduction in risk occurs over the first few iterations with smaller changes in subsequent iterations. The percent change in POF between iterations zero and one, one and two, etc. are 73, 39, 31, 6, 2, 2, respectively. Thus, after iteration four, the percent change in overall POF between iterations is reduced to 2%. The final POF is approximately 11% of the POF from iteration 0.

The red (gray) portion of the column shows the number of new zones created during that iteration and the "blue" portion shows the number of zones retrieved from the previous iteration. The number of zones retrieved is always less than the total number of zones from the previous iteration since parent zones are deleted after being subdivided.

Conclusions

A probabilistically based damage tolerance methodology has been developed in concordance with the Federal Aviation Administration Advisory Circular 33.14-1 to compute the probability of fracture of gas turbine titanium disks subject to low-frequency metallurgical (hard α) defects. This methodology is used during design to augment the traditional safe-life approach and ensure that the risk of fracture due to hard α defects is below a designated design target risk.

This research extends the probabilistically based damage tolerance methodology to ensure that a converged probability of fracture result is obtained that is independent of discretization issues and the experience of the analyst.

The methodology is robust, simple to understand, will converge to the correct solution, and is only weakly dependent on the initial zone discretization. The technique used is akin to "h" refinement in finite element analysis in that a local metric, the risk contribution factor, is used to locate the zones requiring further discretization. These zones are then subdivided about the stress centroid of the zone. Risk results for the new zones are then obtained and combined with the risk from the existing zones.

Efficiency issues are addressed through the use of an automated zone refinement algorithm, an XML-based results database and the parallel processing of zone calculations.

A numerical example of the risk assessment of an impeller is presented. The results are representative of a general application of the algorithm to titanium disks. Four to six iterations are typically sufficient to obtain a reduction in risk of approximately an order of magnitude.

Acknowledgment

This work was performed as part of the Turbine Rotor Materials Design (TRMD) project supported by the Federal Aviation Administration under Cooperative Agreement No. 95-G-041 and Grant No. 99-G-016. The authors would like to acknowledge the collective contributions of the TRMD program team: Southwest Research Institute, General Electric, Honeywell, Pratt & Whitney, Rolls-Royce, the University of Texas at San Antonio, and Mustard Seed Software.

Nomenclature

AC = Federal Aviation Administration Advisory Circular
B = lognormal distribution random variable applied to computed cycles-to-failure
DTR = design target risk
F_i = fracture event of zone i
FAA = Federal Aviation Administration
FE = finite element method
FM = fracture mechanics
hard α = brittle inclusion possibly developed during titanium material melting
life-limiting location = location in the zone with the lowest cycles to failure

n = number of zones
N = cycles to failure
$N(FM)$ = computed cycles to failure from fracture mechanics model
onion skinning = algorithm used to develop a thin layer of elements surrounding the surface
$P[A_i]$ = probability of an anomaly being present in zone i
$P[B_i|A_i]$ = probability of fracture of zone i given an anomaly being present
$P[F_i]$ = probability of fracture event occurring in zone i
POF = Probability of Fracture
R_{cg} = radial coordinate of zone stress centroid
R_{lk} = radial coordinate of node l within element k
RCF = risk contribution factor
S = lognormal distribution random variable applied to driving stress
SIF = stress intensity factor
Z_{cg} = axial coordinate of zone stress centroid
Z_{lk} = axial coordinate of node l within element k
zones = regions of similar cycles to failure
σ = driving stress applied to crack
σ(FE) = driving stress obtained from finite element model
σ_{lk} = hoop stress of node l within element k
δ = distance normal to surface used for onion skinning algorithm

References

[1] NTSB, 1990, "Aircraft Accident Report—United Airlines Flight 232 McDonnell Douglas DC-10-10 Sioux Gateway Airport, Sioux City, Iowa, July 19, 1989," NTSB/AAR-90/06, National Transportation Safety Board, Washington, DC.

[2] Federal Aviation Administration, 2001, Advisory Circular 33.14-1: "Damage Tolerance for High Energy Turbine Engine Rotors," U.S. Department of Transportation, AC, Washington, DC.

[3] Roth, P. G., 1999, "Probabilistic Rotor Design System (PRDS), Gas Turbine Engine Design," Propulsion Directorate, Air Force Research Laboratory, Wright-Patterson Air Force Base, ARFL-PR-WP-TR-1999-2122.

[4] Southwest Research Institute, Allied Signal, General Electric, Pratt and Whitney, Rolls-Royce Allison, Scientific Forming Technologies, 2000, "Turbine Rotor Material Design—Final Report," Federal Aviation Administration, Washington, DC, DOT/FAA/AR-00/64.

[5] Leverant, G. R., Millwater, H. R., McClung, R. C., and Enright, M. P., 2004, "A New Tool for Design and Certification of Aircraft Turbine Rotors," ASME J. Eng. Gas Turbines Power, **126**(1), pp. 155–159.

[6] Enright, M. P., and Huyse, L. J., 2005, "Methodology for Probabilistic Life Prediction of Multiple Anomaly Materials," AIAA J., **44**(4), pp. 787–793.

[7] Downing, S. D., and Socie, D. F., 1982, "Simplified Rainflow Counting Algorithm," Int. J. Fatigue, **4**(1), pp. 31–40.

[8] Subteam to the Aerospace Industries Association Rotor Integrity Subcommittee, 1997, "The Development of Anomaly Distributions for Aircraft Engine Titanium Disk Alloys," *38th AIAA/ASME/ASCE/AHS/ASC Structures, Structural Dynamics, and Materials Conference*, Kissimmee, FL, pp. 2543–2553.

[9] Ang, A. H.-S., and Tang, W. H., 1975, *Probability Concepts in Engineering Planning and Design*, Vol. 1, Wiley, New York.

[10] Wu, Y.-T., Enright, M. P., and Millwater, H. R., 2002, "Probabilistic Methods for Design Assessment of Reliability With INspection," AIAA J., **40**(5), pp. 937–946.

[11] Huyse, L. J., and Enright, M. P., 2003, "Efficient Statistical Analysis of Failure Risk in Engine Rotor Disks Using Importance Sampling Techniques," *44th AIAA/ASME/ASCE/AHS/ASC Structures, Structural Dynamics, and Materials Conference*, Norfolk, VA.

[12] Buecker, H. F., 1970, "A Novel Principle for the Computation of Stress Intensity Factors," Z. Angew. Math. Mech., **50**, pp. 529–546.

[13] Wu, X.-R., and Carlsson, A. J., 1991, *Weight Functions and Stress Intensity Factor Solutions*, Pergamon Press, London.

[14] McClung, R. C., Enright, M. P., Lee, Y.-D., Huyse, L. J., and Fitch, S. H. K., 2004, "Efficient Fracture Design for Complex Turbine Engine Components," ASME Paper No. GT2004-53323.

[15] Momin, F. N., Millwater, H. R., Osborn, R. W., and Enright, M. P., 2004, "Application of a Conditional Expectation Response Surface Approach to Probabilistic Fatigue," *9th ASCE Specialty Conference on Probabilistic Mechanics and Structural Reliability*, Albuquerque.

[16] Momin, F. N., 2004, MS thesis "Application of the Generalized Conditional Expectation Method to Enhance a Probabilistic Design Code," The University of Texas at San Antonio.

[17] Millwater, H. R., Fitch, S. H. K., Enright, M. P., and Huyse, L., 2003, "Application of an XML-Based Database for Probabilistic Analysis," AIAA Paper No. 2003-1837.

[18] Millwater, H. R., Shook, B. D., Guduru, S., and Constantinides, G., 2004, "Application of Parallel Processing to Probabilistic Fracture Mechanics Analysis of Gas Turbine Disks," AIAA Paper No. 2004-1745.